Relationship between Forest Stands Characteristics and NASA/JPL AIRSAR Polarimetric Data Over Mountainous Terrain

Du-Ra Kim* and Kyu-Sung Lee
Inha University, Department of Geoinformatic Engineering
Inchon, KOREA

Abstract

The objective of this study is to analyze the relationship between polarimetric radar backscatters and stand characteristics over the mountainous forest area. L- and P-band full polarimetric airborne SAR data obtained in September 2000 were processed to compare with forest stand maps and ground collected stand variables. After the geometric registration of SAR image, mean radar backscatters were extracted for those ground plots where the stand parameters, such as tree height, DBH, and basal area, were measured during and after the SAR data acquisition. Preliminary analysis was focused on the topographic influence of radar backscattering under the homogeneous forest stand condition. Topographic effects, assessed by the local incidence angles, were different obvious in L-band data while it was not clear with P-band data.

Key words: AIRSAR, Polarization, Forest characteristics, Local incidence angle

Introduction

The estimation of forest stand variables, such as forest type, tree height, diameter at breast height (DBH), basal area, and volume, has been one of major targets in quantitative aspect of active microwave sensing. These stand variables can provide valuable information to diverse applications ranging from natural resource management at local scale to global scale environmental studies.

Unlike optical imagery where the primary source of sensor received signal is from the tree canopy, radar backscattering is well responsive to the physical characteristics of forest stands (Mougin et al.,1999). During the last two decades, there were several studies to define the relationship between stand characteristics and radar backscattering with different frequency. In recent years, multi-polarization SAR data have been introduced to forest environments (Sheen et al., 1992).

Most forests in Korea are found in

mountainous terrain. Radar backscattering coefficients are greatly influenced by the geometric configuration between radar antenna and terrain slope (Menges et al., 2001). Although there have been many attempts to define the relationship between polarimetric radar returning and forest stand variables, the study sites were mostly the forest land located in relatively flat area. In this study, we are attempting to define the topographic effects on the radar backscattering over forest land in mountainous terrain.

Study Area and Ground Data Collection

We used NASA/JPL AIRSAR L- and P-band full polarimetric data. The AIRSAR polarimetric data were acquired on September 30, 2000 during the PacRim II mission (table 1). The study area is located in Unyang, Kyungsang Province of the southeastern part of Korea and covers approximately 10x20Km^2. This area is mostly hilly terrain covered by forests. The forest in the area consisted of temperate deciduous species and relatively young plantation stand of pitch pine (*Pinus rigida*) and Korean pine (*Pinus koraiensis*).

Extensive ground measurements were conducted over the study sites during the fall of 2000 and 2001. Dominant tree species, tree height, and DBH were measured and verified at 78 ground stands (figure 1). Each sample forest stand has very homogeneous stand structure within it. The 78 sample stands were chosen to represent diverse group of forest types and tree size. Global positioning system (GPS) was used to find the exact location of every ground plot. In addition to the ground measurements, we used the forest stand map over the study area to collect and to verify the additional stand characteristics. The forest stand maps were produced by the national forest inventory work in 1998 and showed rather detailed information on the stand. The forest stand map, produced by 1:15,000 scale aerial photograph and ground verification, shows the forest type and other stand characteristics such as stock density, mean DBH, and stand age.

Table 1. Characteristics of NASA AIRSAR data.

Data acquisition date	September 30, 2000
Wavelength	L(23.5cm), P(68cm)
Polirization	HH, VV, HV, VH full
Flight altitude	7401.6m
Incidence angle	28.2~64.1 degree
Pixel space	5m

Figure 1. TM image of the Study area showing the location of ground sample plots.

Methods

JPL AIRSAR provided L-band and P-band polarimetry data in the compressed Stoke matrix format (van Zyl and Ulaby, 1990). Four bands of full polarization data expressed by radar backscattering coefficients were generated from the compress Stoke matrix. Along with the polarimetry data, NASA/JPL also supplied the digital elevation model (DEM) data derived from C-band interferometry, the local incidence angle map derived from DEM, the normalized correlation coefficient map between the two C-band interferometric bands.

Total eight bands of L-band and P-band polarimetry data were initially georectified to the regional plane rectangular coordinate system using a set of ground control points (GCP). During the geometric correction process, Landsat ETM+ data and other AIRSAR products, such as the local incidence angle map, DEM, and correlation coefficient map, were also registered to the same coordinate system. The local incidence angle map was particularly important to analyze the topographic effect. The incidence angle is defined as the angle between the normal to a surface and the radar look direction and reflects the geometric relationship of the terrain slope and aspect of each pixel position.

Speckle noise in SAR data can be often obstacle to extract accurate information of the target of interest. For this study, we used the enhanced Frost filter to reduce speckle noise in multiple polarimetry data (Frost et al., 1982).

Radar backscattering coefficients corresponding to the ground sample plots were extracted from the eight polarimetric bands and the local incidence angle map. Each ground plot having relatively homogeneous stand characteristics covers an area of about $10x10m^2$. Beside the ground plots that were actually visited, we added more sample plots by using the forest stand map. The digital map of forest stand was overlaid to the color composite images of georectified Landsat TM and multi-polarimetirc data. From the interpretation of color composite images overlaying with the forest stand map, we were able to select about 400 additional plots of known forest stand characteristics. Within the boundary each sample plots, all pixel values (backscattering coefficient) were extracted and their mean value was obtained for each plot.

To analyze the topographic effect on radar backscattering over mountainous forest, we selected mature stands of pine and mixed deciduous and coniferous forest. 23 plots of pine stands have similar stand characteristics (18~28cm of DBH, 31~40 years old, medium density) and are distributed on diverse topographic positions). 85 plots of mixed species of deciduous and coniferous stands have relatively young and small trees (6~16cm of DBH, 21~30 years, high density).

Along with the analysis of topographic effects, we also try to compare the magnitude of backscattering coefficients among different forest type. Assuming that the topographic influence might overpower the stand characteristics, the sample plots used for this study were limited to those ones under the same local incidence angle group. The local incidence angle map was reclassified into 18 categories by 10 degrees range.

Mean radar backscattering coefficients among the different forest types were compared within the same incidence angle category.

Results and Discussion

Figure 2 shows the relationship between multipolarized radar backscatters and local incidence angle from the 23 relatively homogeneous pine stands in L-band and P-band. In L-band data, it is clear that backscattering coefficients tend to decrease at the incidence angles larger than 90 degrees. However, no such relationship is obvious in P-band data regardless of polarization. Also, the topographic effects are a little clear with cross-polarizaton (VH, HV) data as compared to co-polarization data.

Figure 3 shows about the same relationship found in figure 2. It uses 85 sample plots of relatively homogeneous stands of mixed deciduous and coniferous species. The local incidence angle effect can only be seen in L-band polarization data. Backscattering coefficients decrease at the incidence angle larger than 90 degree while they tend to stable within the incidence angles from 0 to 90 degree.

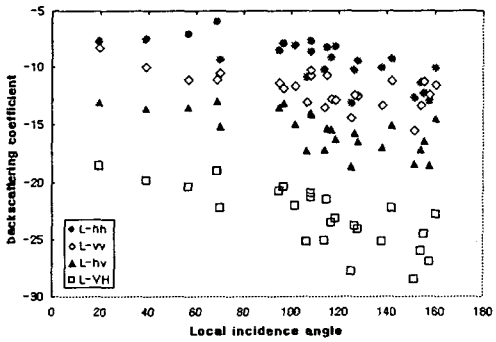

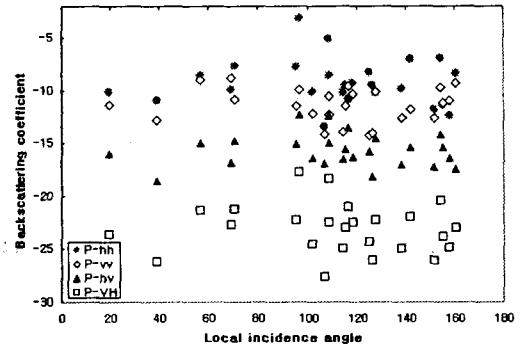

Figure 2. Relationship between radar backscatters and the local incidence angle from relatively homogeneous pine stands (DBH:18~28cm, age:31~40 year, stock density: middle) in L-band (top) and P-band (bottom).

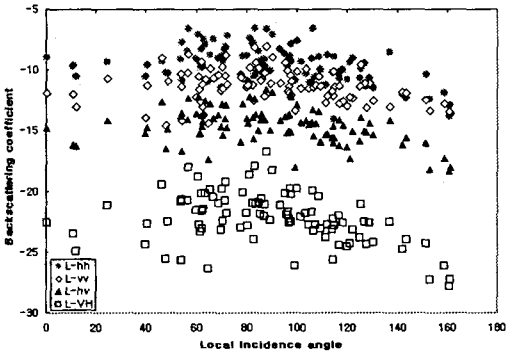

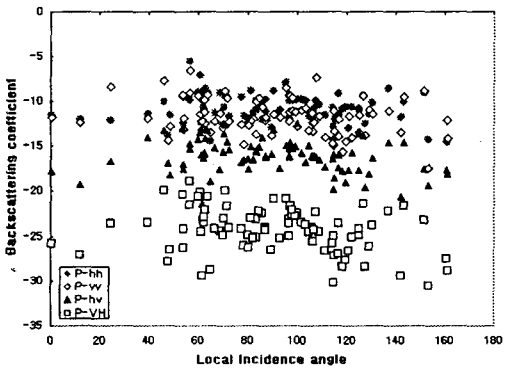

Figure 3. Relationship between radar backscatters and the local incidence angle from relatively homogeneous stands of deciduous species (DBH: 6~16cm, age: 21~30 year, stock density: high).

The difference of the topographic effect between L-band and P-band polarimetric data can be also seen from the imagery. Figure 4 shows the gray scale images of color composite of L-band and P-band multi-polarization data. The tonal contrast between the antenna facing slope and the antenna opposite slope is much clear with L-band image. Such tonal variation diminishes in P-band image.

(a)

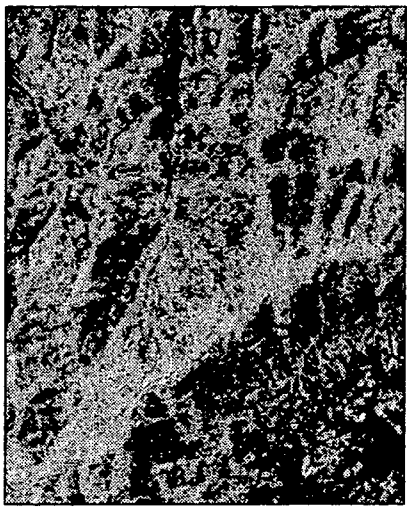

(b)

Figure 4. Topographic effects between L-band L-band (a) and P-band (b) images (gray scale image of color composite - R: HH, G: VV, B: HV).

Figure 5 shows the mean backscattering coefficients of four different forest types by L- and P-band polarimetric band. To avoid any other stand characteristics beside the forest type, these sample stands have similar stand age, DBH group, and stand density. Although the differences of mean backscattering coefficients are not much different among the four types, L-band polarimetric bands are better to differentiate forest types than P-band data. In particular, natural coniferous stands have rather distinct from other forest types at L-band polarization regardless of incidence angle. Plantation pine type is well separated at the L-band 30-40 incidence angle category.

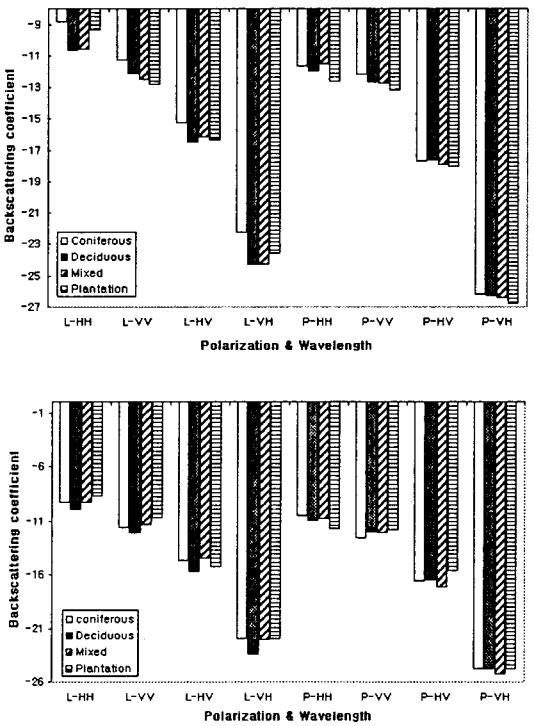

Figure 5. Mean backscattering coefficients among the four different forest types in which those sample stands were selected within the same local incidence angle category of 30degree to 40degree (top) and 70degree to 80degree (bottom).

Conclusion

There has been certain limitation to use SAR data to characterize forest stand in hilly terrain. In this paper, we analyzed L-band and P-band multiple polarimetry data over mountainous forest. From the preliminary analysis on the local incidence angle effects, we can conclude as follows:

- The topographic effect is more obvious in L-band cross-polarimetry data than in P-band and L-band co-polarimery data. Since the P-band polarimetric data show less influence by topography, they may be more appropriate to acquire the physical characteristics of forest stand in hilly terrain.
- Under the similar local incidence angle, forest types can be better separated with L-band polarimetry data.

References

Sheen, Dan R. and Linda P.Johnston, 1992, "Statistical and Spatial Properties of Forest Clutter Measured with Polarimetric Synthetic Aperture Radar(SAR)". IEEE Tansactions on Geoscience and remote Sensing, 30(3), 578-588

Menges, C. H., J. J. Van Zyl, C. J. E. Hill and W. Ahmad, 2001, "A procedure for the correction of the effect of variation in incidence angle on Airsar data". International Journal of Remote Sensing, Vol(22), No(5), pp 829-841.

Mougin, E., C. Proisy, G. Marty, F. Fromard, H. Puig, J. L. Betoulle and J. P. Rudant, 1999, "Multifrequency and Multipolarization Radar Backscattering from Mangrove Forests". IEEE Tansactions on Geoscience and remote Sensing, Vol, 37, No. 1. pp 94-102

J. J. van Zyl and F. T. Ulaby, 1990 "Scattering Matrix representations for simple targets", Radar polarimetry for Geoscience Applications, Artech House, Norwood, MA, pp. 17-52

Frost, V.S., J.A. Stiles, K.S. Shamugan, and J.C. Holtzman, 1982, "A Model for Radar Images and its Application to Adaptive Digital Filtering of Multiplicative Noise", IEEE Transactions Pattern Analysis and Machine Intelligence, Vol 4, No 2, pp.157-166

AIRSAR Homepage : http://airsar.jpl.nasa.gov